

# REDESIGN OF CERN'S QUADRUPOLE RESONATOR FOR TESTING OF SUPERCONDUCTING SAMPLES

V. del Pozo Romano\*<sup>1</sup>, F. Gerigk, R. Betemps, R. Illan Fiastre and T. P. Mikkola  
 CERN, Geneva, Switzerland  
<sup>1</sup>also at Ciemat, Madrid, Spain

## Abstract

The quadrupole resonator (QPR) was constructed in 1997 to measure the surface resistance of niobium samples at 400 MHz, the technology and RF frequency chosen for the LHC. It allows measurement of the RF properties of superconducting films deposited on disk-shaped metallic substrates. The samples are used to study different coatings which is much faster than the coating, stripping and re-coating of sample cavities. An electromagnetic and mechanical re-design of the existing QPR has been done with the goal of doubling the magnetic peak fields on the samples.

Electromagnetic simulations were carried out on a completely parametrized model, using the actual CERN's QPR as baseline and modifying its dimensions. The aim was to optimize the measurement range and resolution by increasing the ratio between the magnetic peak fields on the sample and in the cavity. Increasing the average magnetic field on the sample leads to a more homogenous field distribution over the sample, which in turn gives a better resolution. Some of the modifications were based on the work already done by Helmholtz-Zentrum-Berlin for their upgraded version of the QPR.

## DESCRIPTION

The QPR consists of a screening cavity made by two separate cans and four vertical rods supported from the top-plate that are bent at the end into half ring pole shoes (see Fig. 1) [1]. The loop formed by the two pole shoes is placed 0.7 mm above the sample disk and focusses the RF field to its surface. The resonance inside the cavity occurs because the length of the rods plus the gap between them and the sample is  $\lambda/2$  of the operation frequency of 400 MHz, although it was also refurbished in 2009 for operation at 800 MHz and 1.2 GHz [2]. The sample is welded to a niobium cylinder that is inserted from below into the resonator, leaving a gap between them. This can be compared to a coaxial line where the inner cylinder is thermally decoupled from the resonator and also higher modes than the quadrupole mode are in cut off within the gap.

The measurement of the surface resistance is done by a calorimetric method. The advantages of this technique is the high sensitivity and the independence from a reference sample. The resonator is immersed in an helium bath that also flows inside the hollow rods. As the fields decay on the gap, the cylinder is only heated on the sample's surface. Below the sample's disk a heater is attached and used to change its temperature, also four temperature sensors are placed under the regions of high magnetic field. Once the temperature

is stabilized with the DC heater, the RF is turned on and the power of the heater is lowered until reaching the initial temperature. The power dissipated by RF is the difference

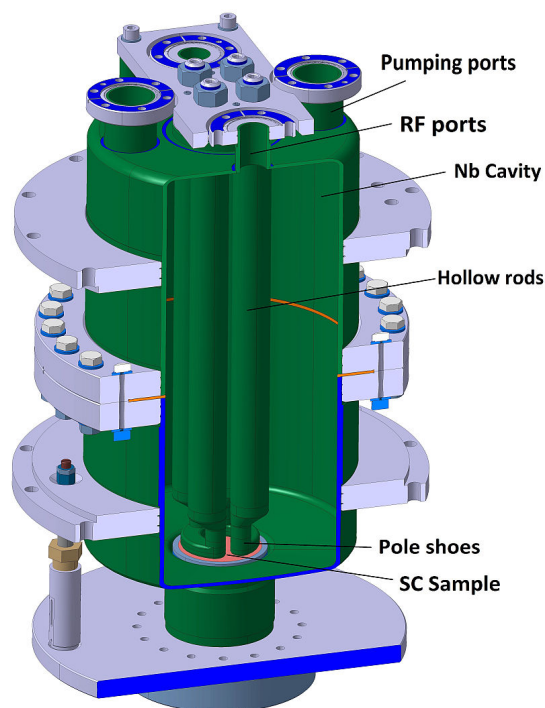


Figure 1: 3D view of the quadrupole resonator as prepared for fabrication.

between the DC power applied without RF,  $P_{DC1}$  and the DC power applied with RF  $P_{DC2}$ . Assuming the surface resistance  $R_S$  to be constant over the sample surface area and independent of the magnetic field, the surface resistance can be calculated as the power dissipated divided by the integrated magnetic field over the sample surface [3, 4].

$$R_S = \frac{2 \cdot (P_{DC1} - P_{DC2})}{\int_{Sample} |\vec{H}|^2} \quad (1)$$

## RF OPTIMIZATION

The aim of this study was to optimize the size and parameters of the Quadrupole Resonator (QPR) at CERN, in order to maximize some figures that define the performance of the QPR as they are related to thermal quenches that limit the peak magnetic field on the sample to 60 mT, field emission, multipacting and microphonics when operated at 800 and 1200 MHz [5].

\* veronica.del.pozo.romano@cern.ch

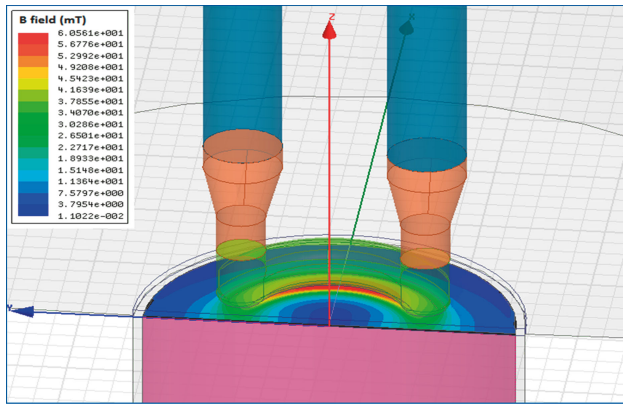


Figure 2: Magnetic field on sample's surface.

- $B_s/B_{pk}$  and  $B_s/E_{pk}$  relate the peak magnetic field on the sample ( $B_s$ ) with the peak magnetic field on the pole shoe ( $B_{pk}$ ) (see Fig. 2) and the peak electric field on the rods ( $E_{pk}$ ). Increasing these parameters lowers the risk of quenches and enhanced field emission.
- $\frac{\int_S H \cdot dS}{S_{sample}}$  the average magnetic field on the sample is the surface integral of the H field on the sample divided by the sample's surface and determines the homogeneity of the field distribution. Increasing this parameter increases the resolution of the measurements.
- The parameter  $B_{edge}$  determines the maximum B field at any point on the sample's edge. The leakage of field on the coaxial gap cannot be too high as it heats the sample's cylinder.

The original QPR was fabricated using niobium of different RRR for each part (RRR40 for the cavity, RRR100 for the rods and RRR250 for the pole shoes). The first change with respect to the original QPR is that it will be completely fabricated in Nb RRR300 (cavity, rods and pole shoe).

### Simulations

First, the original design was modelled and completely parametrized in HFSS. It was important to find a suitable mesh, in particular for the gap between the loop and the sample surface, that would not take too much computing time. To save resources, only a quarter of the QPR and symmetry planes were necessary in order to simulate the complete structure.

Different parameters were modified to study their effect on the fields distribution. Some of these effects were already analysed by HZB [4]. Reducing the gap distance and increasing the rod radius improve the measurement range, as in Figures 3 and 4. This is due to the increase in the peak magnetic field focussed on the sample when the gap is reduced and to the decrease on the electric field on the rods when their diameter is increased. The peak in the second plot corresponds to the point where a further increase of the diameter will place the rods too close to each other increasing the electric field. Modifying the width of the pole shoes improves the field distribution over the sample, Figure 5 shows the distribution of the magnetic field along

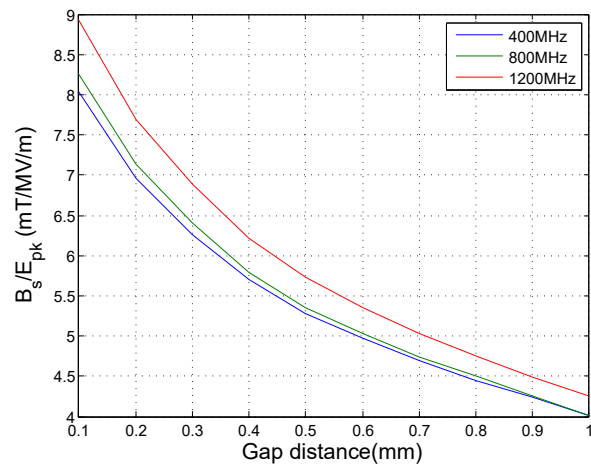


Figure 3: Measurement range  $B_s/E_{pk}$  vs. gap distance.

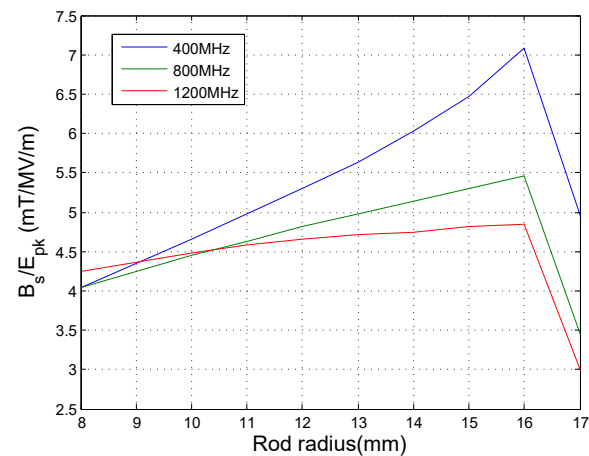


Figure 4: Measurement range  $B_s/E_{pk}$  vs. rod's diameter.

the axis of the sample passing through the spot of maximum field. The field is better spread over the sample in the new design, increasing the average field on the surface and thus, the resolution of the measurements. The height of the rods and the cavity are modified for re-tuning.

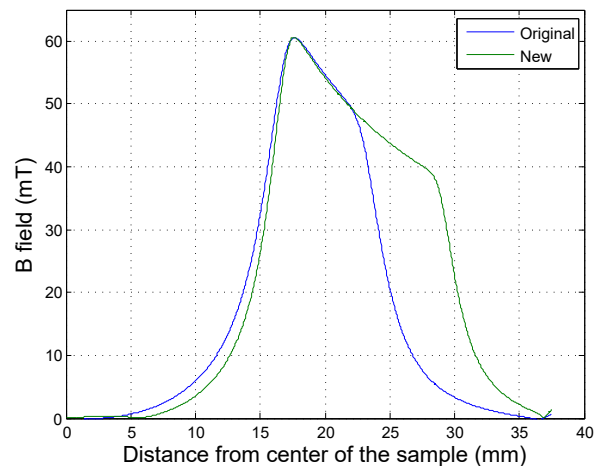


Figure 5: B field on the axis of the sample, normalized to a maximum field of 60 mT.

Content from this work may be used under the terms of the CC BY 3.0 licence (© 2017). Any distribution of this work must maintain attribution to the author(s), title of the work, publisher, and DOI.

## Results

The most important modifications are shown in Figure 6, and the field results for the three resonant frequencies are compared in Table 1 for the original and new design. By reducing the gap distance the field illuminated in the sample is higher, and thus is the ratio  $H_{ss}/H_{pk}$ . The increase in the diameter of the rods leads to an electric field more diluted in the rod's surface and therefore the ratio  $B_{ss}/E_{pk}$  also increases.

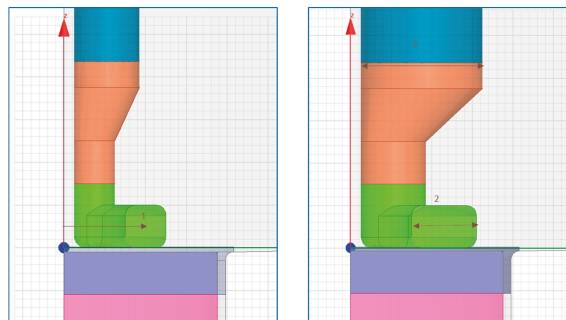


Figure 6: Original and new pole shoe geometry.

Table 1: Field Results for the Three Modes

Figure	Original design	New design
Res. Freq. [MHz]	399.7 / 803.3 / 1211	398.1 / 806.2 / 1224
$H_{ss}/H_{pk}$	0.87	0.91
$B_{ss}/E_{pk}$ [mT/MV/m]	4.00 / 4.00 / 4.22	5.28 / 5.28 / 5.40
Av. field on surface [mT]	16.4	22.5
$B_{edge}$ [mT]	1.5	2.5

## ALIGNMENT OF THE SAMPLE

To calculate the field distribution from the measured temperature variations, the QPR needs to be calibrated. For the calibration two field relations need to be known in advance from software simulations:

$$\frac{H_{pk}}{\int_{Sample} H \cdot dS} \quad \text{and} \quad \frac{H_{pk}^2}{U}$$

being  $U$  the stored energy in the cavity. To solve them it is very important that the geometry of the QPR corresponds exactly to the simulations. Therefore, the position of the sample inside the QPR needs to be very precise, not only its distance with the pole shoes but also its inclination (see Fig. 7). This inclination could be produced either by a tilt in the welding of the rods to the top plate of the cavity or by the mounting of the sample inside the cavity.

Measurements were done to know the variations in the alignment of the sample due to the mounting process. They showed that the inclination of the sample only varied a few microns but the gap distance could vary up to 67  $\mu\text{m}$ . The resonance frequency varies as a function of this distance, as shown in Table 2, so it is possible to calculate it by measuring the frequency and then to correct it. Neither the original QPR nor the HZB one have a system that allows a precise correction of this distance, therefore a new alignment system

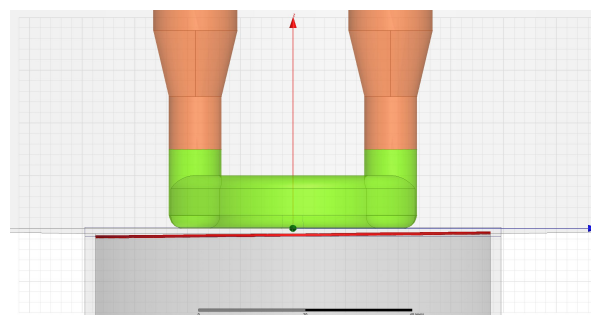


Figure 7: Possible sample's misalignment.

is being developed to correct the gap distance while maintaining the alignment of the sample with respect to the pole shoes.

Table 2: Resonant Frequency Variation vs. Gap Distance

Mode	Variation
400 MHz	$\sim 0.8$ MHz/100 $\mu\text{m}$
800 MHz	$\sim 1.2$ MHz/100 $\mu\text{m}$
1200 MHz	$\sim 1.7$ MHz/100 $\mu\text{m}$

## CONCLUSION AND FUTURE WORK

The QPR has been redesigned in order to achieve higher magnetic field and better field distribution on the sample surface and it is ready for its fabrication at CERN. Last modifications are being done to the mechanical drawings for their approval and the niobium has already been purchased. A last step pending is the final design of the alignment system and the design of the couplers and pick-up antenna.

## ACKNOWLEDGEMENTS

The authors would like to thank S. Aull and HZB for sharing their knowledge about the Quadrupole Resonator, as well as the workshop at CERN for their inputs regarding the fabrication process.

## REFERENCES

- [1] E. Mahner, S. Calatroni, E. Chiaveri, E. Haebele, and J. M. Tessier, "A new instrument to measure the surface resistance of superconducting samples at 400 MHz", *Rev. Sci. Instrum.*, 74(7):3390, 2003.
- [2] T. Junginger, W. Weingarten, and C. Welsch, "Extension of the measurement capabilities of the quadrupole resonator", *Rev. Sci. Instrum.*, 83:063902, 2012.
- [3] S. Aull, S. Doebert, T. Junginger, and J. Knobloch, "High resolution surface resistance studies", *Proc. 6th Int. Conf. on RF Superconductivity (SRF'13)*, Paris, France, September 2013, paper WEIOC01, pp.785-788.
- [4] R. Kleindienst, O. Kugeler, J. Knobloch, "Development of an Optimized Quadrupole Resonator at HZB", in *Proc. 6th Int. Conf. on RF Superconductivity (SRF'13)*, Paris, France, September 2013, paper TUP074, pp.608-610.
- [5] T. Junginger, "Investigation of the Surface Resistance of Superconducting Materials", PhD thesis, University of Heidelberg, Germany, July 2012.